

Building a cell cycle oscillator: hysteresis and bistability in the activation of Cdc2

Joseph R. Pomerening*, Eduardo D. Sontag† and James E. Ferrell Jr*‡

*Department of Molecular Pharmacology, Stanford University School of Medicine, Stanford, CA 94305-5174, USA

†Department of Mathematics, Rutgers University, New Brunswick, NJ 08903, USA

‡e-mail: james.ferrell@stanford.edu

Published online: 10 March 2003; DOI: 10.1038/ncb954

In the early embryonic cell cycle, Cdc2–cyclin B functions like an autonomous oscillator, whose robust biochemical rhythm continues even when DNA replication or mitosis is blocked¹. At the core of the oscillator is a negative feedback loop; cyclins accumulate and produce active mitotic Cdc2–cyclin B^{2,3}; Cdc2 activates the anaphase-promoting complex (APC); the APC then promotes cyclin degradation and resets Cdc2 to its inactive, interphase state. Cdc2 regulation also involves positive feedback⁴, with active Cdc2–cyclin B stimulating its activator Cdc25 (refs 5–7) and inactivating its inhibitors Wee1 and Myt1 (refs 8–11). Under the correct circumstances, these positive feedback loops could function as a bistable trigger for mitosis^{12,13}, and oscillators with bistable triggers may be particularly relevant to biological applications such as cell cycle regulation^{14–17}. Therefore, we examined whether Cdc2 activation is bistable. We confirm that the response of Cdc2 to non-degradable cyclin B is temporally abrupt and switch-like, as would be expected if Cdc2 activation were bistable. We also show that Cdc2 activation exhibits hysteresis, a property of bistable systems with particular relevance to biochemical oscillators. These findings help establish the basic systems-level logic of the mitotic oscillator.

It has been known for thirty years that there is an autocatalytic element to activation of the M-phase trigger. Microinjection of cytoplasm from M-phase *Rana pipiens*⁴ or *Xenopus laevis*^{18,19} oocytes causes G2-phase oocytes to enter M phase. Furthermore, microinjection of cytoplasm from these M-phase oocytes causes progesterone-naïve G2-phase oocytes to enter M phase, and the titre of the mature oocytes' M-phase promoting factor (MPF) activity never decreases with sequential cytoplasmic transfer⁴. The basic mechanisms of this autocatalysis were defined through experiments with *Xenopus* egg extracts treated with recombinant, non-degradable cyclins²⁰. Cyclin-induced activation of Cdc2 inactivates the kinases that inhibit Cdc2 activity and activates the phosphatase that dephosphorylates the same target residues²⁰. Subsequent work established that Cdc2 can activate its activator Cdc25 (refs 5–7) through the intermediacy of the Polo-like kinase Plx1 (refs 21, 22), and that Cdc2 can inactivate its inactivators Wee1 and Myt1 (refs 8–11).

It was realized that these positive feedback loops — Cdc2-mediated activation of Cdc25 and inactivation of Wee1 and Myt1 — could function as a bistable system^{12,13}, toggling between two discrete alternative stable steady states. Systems are termed bistable if they toggle between two discrete alternative states without being able to rest in intermediate states (Fig. 1c). In this case, the two stable states are interphase, in which Cdc2 and Cdc25 are inactive and Wee1 and Myt1 are active, and the early part of mitosis (up to anaphase), in which Cdc2 and Cdc25 are active and Wee1 and Myt1 are inactive. Bistability is not an inevitable consequence of positive

feedback²³, nor is it the only useful systems-level property that can arise from positive feedback loops (for example, sensitivity amplification²⁴ is a more robust property of positive feedback systems than bistability is). Nevertheless, a bistable trigger could be critical for mitotic oscillator function by ensuring that a cell settles in discrete, mutually exclusive interphase and M-phase states and not in a continuum of intermediate states^{12,13}. Bistability could also help keep a cell from slipping rapidly back and forth between cell cycle phases ('chattering') during transitions into and out of mitosis¹³.

Moreover, bistability is one way to ensure that a mitotic oscillator will never approach a stable steady-state, but will instead oscillate indefinitely, and an oscillator that possesses a bistable trigger — a relaxation oscillator, similar in its basic mechanism to the Van der Pol oscillator from electrical engineering and the FitzHugh/Nagano oscillator from ecology — has a number of distinctive properties. A simple two-component negative feedback system, such as one in which Cdc2–cyclin B directly activates the APC and the APC in turn directly inactivates Cdc2–cyclin B, will inevitably approach a stable, intermediate steady state (Fig. 1d, e; also see Supplementary Information Part 1 for a mathematical demonstration). Some aspect of the circuit must be altered to convert it into a satisfactory oscillator. One way is to add another component to the feedback loop; for example, an intermediary, such as Plx1, between active Cdc2 and the APC (Fig. 1f). The resulting regulatory circuit can exhibit sustained negative feedback oscillations (Fig. 1g), and an oscillator of this class could in principle be the basis of the early embryonic cell cycle^{12,25}. A different way of producing sustained oscillations is to add a bistable trigger to a negative feedback loop, resulting in a relaxation oscillator (Fig. 1h, i). This type of oscillator may have advantages over simple negative feedback oscillators in terms of noise rejection, reliability, self-synchronization and spatial propagation^{14–16}, and may be particularly suitable as a biological timer.

Therefore, we wanted to determine experimentally whether the Cdc2 system is actually bistable. We began by examining the time course of Cdc2 activation by a non-destructible *Xenopus* B-type cyclin, $\Delta 65$ -cyclin B1, in undiluted, cycloheximide-treated interphase *Xenopus* egg extracts lacking endogenous cyclins (the non-destructible cyclin is not subject to APC-mediated proteolysis, allowing an examination of Cdc2 responses to specific, unchanging cyclin concentrations). If activation of Cdc2 is bistable, then the time course of Cdc2 activation in response to a constant level of non-degradable cyclin should exhibit a temporal lag that precedes an abrupt transition between low and high Cdc2 activity, as autocatalysis means that the rate of Cdc2 activation will increase as Cdc2 activity increases. The activation of Cdc2 was temporally abrupt and reached an apparent steady state within approximately 60 min (Fig. 2a), as previously reported for activation of *Xenopus* Cdc2 by a non-degradable sea urchin cyclin protein in extracts²⁰. The observed temporal abruptness is consistent with the predicted

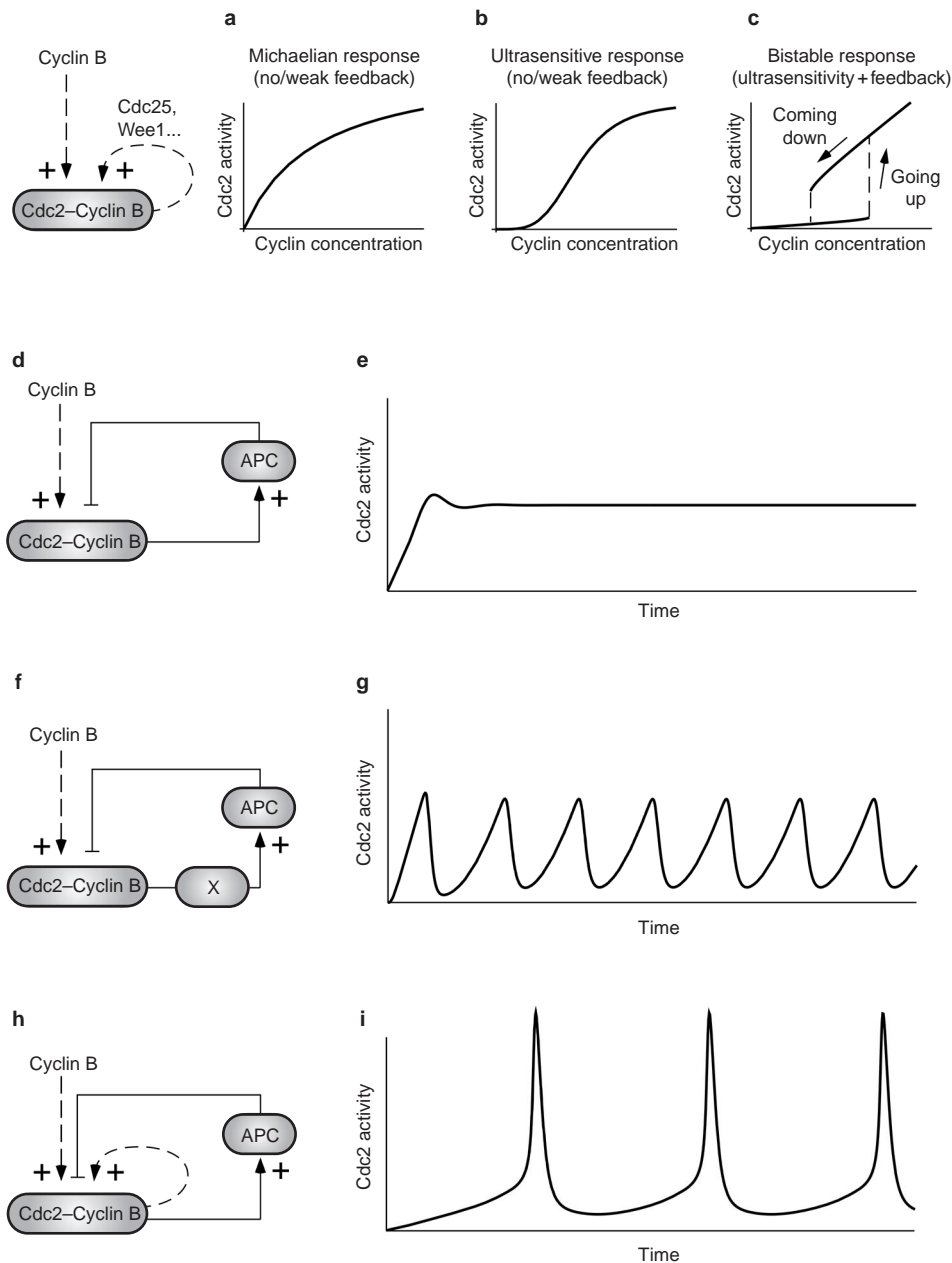


Figure 1 Expected behaviours of several plausible Cdc2-APC circuits.

a-c, Three ways that Cdc2 could respond to different concentrations of non-degradable cyclin in the absence of the APC. The Michaelian response (**a**) would be expected if cyclin directly activated Cdc2. The ultrasensitive response (**b**) could arise from multistep activation mechanisms, from stoichiometric inhibitors or from saturation effects. The bistable response (**c**) could arise from a combination of ultrasensitivity and positive feedback. **d-i**, Three ways that a Cdc2-APC circuit could respond to a constant rate of cyclin synthesis. If the response of Cdc2 to

cyclin is Michaelian or ultrasensitive (as in **a** and **b**) and the regulation of the APC by Cdc2 is direct, then the system will always approach a stable steady state (**d**, **e**). Adding an intermediate enzyme (such as Plx1) between Cdc2 and the APC can turn a monostable system (as in **d** and **e**) into a negative feedback oscillator (**f**, **g**). Adding positive feedback to make the response of Cdc2 to cyclin bistable (as in **c**) can turn the system into a relaxation oscillator, with explosive spikes of Cdc2 activity (**h-i**). Details of the modelling can be found in Supplementary Information, Part 3.

behaviour of a bistable system, although temporal abruptness can also be detected in a highly switch-like, but monostable, system (one that is highly cooperative or ultrasensitive (Fig. 1b), but not bistable (Fig. 1c)).

In addition, if activation of Cdc2 is bistable, there should be a discontinuity in the steady-state level of Cdc2 activity as a function of added $\Delta 65$ -cyclin B1 concentration. As previously reported for activation of Cdc2 by sea urchin cyclin²⁰, small changes in cyclin

concentration result in large changes in Cdc2 activity (Fig. 2b). These data are consistent with a bistable response — there could be a discontinuity in the stimulus/response curve — but again the data are also compatible with a highly switch-like, ultrasensitive monostable response.

A more definitive way of distinguishing between monostable and bistable responses is to try and detect hysteresis — a distinctive splitting of the stimulus-response relationship — in the response

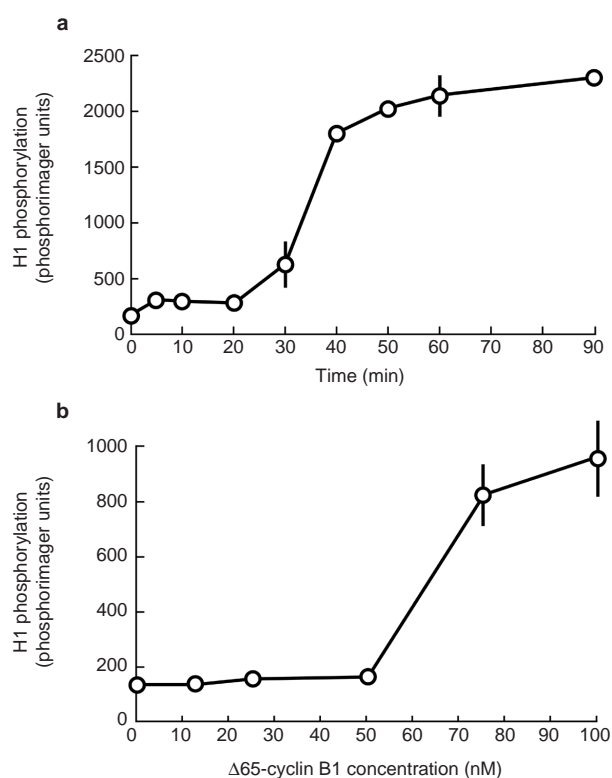


Figure 2 Cdc2 activation in interphase extracts treated with $\Delta 65$ -cyclin B1. **a**, Time course of Cdc2 activation. Extracts were treated with a supra-threshold concentration of $\Delta 65$ -cyclin B1 (200 nM) and the resulting Cdc2 activity was measured as a function of time. Data are shown as means \pm s.e.m. for three replicates. **b**, Steady-state Cdc2 activity as a function $\Delta 65$ -cyclin B1 concentration. Data are shown as means \pm s.e.m. for three replicates. The data are consistent with an ultrasensitive response that is monostable and continuous (with a Hill coefficient of approximately 10), or one that is discontinuous and bistable.

of Cdc2 to $\Delta 65$ -cyclin B1. For a given fixed concentration of $\Delta 65$ -cyclin B1, a monostable system will approach one particular steady-state level of Cdc2 activity regardless of the system's history (Fig. 1a, b). In contrast, a bistable system has the potential to approach either of two different stable steady-states, depending on the history of the system. The stimulus–response curve for a bistable system should exhibit hysteresis, with a relatively high threshold for switching from interphase to M phase, and a lower threshold for switching from M phase back to interphase (Fig. 1c). Thus, if the Cdc2 system is bistable, there should be concentrations of $\Delta 65$ -cyclin B1 that are not sufficient to drive an interphase extract into M phase, but are sufficient to maintain an M-phase extract in M phase for long periods of time.

To experimentally determine whether the response of Cdc2 to $\Delta 65$ -cyclin B1 exhibited hysteresis, we prepared M-phase extracts (also termed cytotostatic factor (CSF) extracts) from unfertilized *Xenopus* eggs and split them into two aliquots (Fig. 3a, b). One aliquot was incubated with calcium (1 mM) for 30 min to trigger cyclin destruction and drive the extract into interphase. Various concentrations of $\Delta 65$ -cyclin B1 were then added to this interphase extract and Cdc2 H1 kinase activity was assessed every 15–30 min (Fig. 3a). An apparent steady state was reached within 60–90 min (data not shown), allowing the steady-state level of Cdc2 activity to be determined for a given concentration of $\Delta 65$ -cyclin B1 in an extract coming from interphase (Fig. 3a, c–g; going up). The other aliquot of M-phase extract was incubated with various concentrations of $\Delta 65$ -cyclin B1 for 30 min to allow excess endogenous Cdc2 to bind the non-degradable cyclin and become activated. The

extract was then incubated with calcium to trigger destruction of the endogenous cyclin (Fig. 3b). Again, an apparent steady state was reached within 60–90 min, allowing us to determine the steady-state level of Cdc2 activity for a given concentration of $\Delta 65$ -cyclin B1 in an extract coming from M phase (Fig. 3b–g; coming down).

At 45–60 nM $\Delta 65$ -cyclin B1, there seemed to be two distinct alternative steady states for the Cdc2 system, depending on whether it was going up from interphase or coming down from M phase (Fig. 3c). Cyclin concentrations in this range were able to sustain the elevated Cdc2 activities of M-phase extracts for long periods of time, but were unable to significantly increase Cdc2 activities in interphase extracts (Fig. 3c). Thus, activation of Cdc2 does exhibit hysteresis, supporting the hypothesis that the mitotic trigger is bistable.

Next we assessed whether the differences in Cdc2 activity present in the on state (Fig. 3c, upper curve) versus the off state (Fig. 3c, lower curve) had significant effects on the biochemistry and cell biology of the extracts. Therefore, we assessed the phosphorylation states of Cdc25 (Fig. 3d), Wee1 (Fig. 3e) and p42 mitogen-activated protein kinase (MAPK; Fig. 3f) in the two types of extracts. In M-phase extracts and M-phase embryos, all three proteins are known to become hyperphosphorylated and shift to a higher apparent molecular mass on immunoblots. These shifts can therefore be used as biochemical markers of whether an extract is in an M-phase-like state. Concentrations of $\Delta 65$ -cyclin B1 between 45 and 60 nM did not cause mitotic hyperphosphorylation of Cdc25, Wee1 or p42 MAPK when the extract was coming out of interphase (Fig. 3d–f, going up), but did sustain their mitotic hyperphosphorylation when the extract was coming out of M phase (Fig. 3d–f, coming down). Hysteresis can also be assessed morphologically using added sperm chromatin to determine whether an extract is in interphase (chromatin decondensed, nuclear envelope intact) or M phase (chromatin condensed, nuclear envelope dissolved). Addition of 45–60 nM $\Delta 65$ -cyclin B1 did not induce chromatin condensation or nuclear envelope breakdown in interphase extracts, but did sustain chromatin condensation and nuclear envelope breakdown in M-phase extracts (Fig. 3g). Thus, the quantitative differences in the Cdc2 activity responses of mitotic and interphase extracts are significant and result in qualitative differences in the cell cycle phase of the extract, as assessed by biochemical and morphological analysis.

One trivial explanation for these findings could be that different levels of cyclin protein were present in the 'going up' and 'coming down' extracts, either because the endogenous cyclin was not completely degraded in the 'coming down' extracts, or because the $\Delta 65$ -cyclin B1 was unstable in the 'going up' extracts. To test this, we used ^{35}S -methionine to metabolically label cyclins in a CSF-arrested extract and then examined the disappearance of the ^{35}S -labelled cyclins as a function of time after calcium treatment. All of the detectable cyclin bands were rapidly degraded (Fig. 3h), suggesting that cyclin destruction was complete and that undegraded endogenous cyclin did not account for the elevated Cdc2 activity detected in the 'coming down' extracts. To ensure that $\Delta 65$ -cyclin B1 was not unstable in the 'going up' extracts, we added trace amounts of ^{35}S -labelled *in-vitro*-translated $\Delta 65$ -cyclin B1 to interphase extracts treated with or without additional unlabelled $\Delta 65$ -cyclin B1 before examining its degradation. We found no measurable degradation of $\Delta 65$ -cyclin B1 over a 90-min incubation in either type of extract (see Supplementary Information, Fig. S2). Taken together, these experiments demonstrate that the observed hysteresis was not caused by problems with the degradation of endogenous cyclin B1 or the stability of exogenous $\Delta 65$ -cyclin B1.

Next, we asked whether hysteresis is a special property of the cell cycle stages examined in Fig. 3, or is also present in later cell cycles. Thus, we prepared cycling egg extracts²⁶ and verified morphologically that they underwent multiple rounds of mitosis (Fig. 4a, top). We also verified that addition of cycloheximide at the time of the first mitotic M phase (50 min) resulted in arrest of the extract in interphase (Fig. 4a, bottom). We then compared the amount of $\Delta 65$ -cyclin B1 required to drive a *Xenopus* egg extract from this

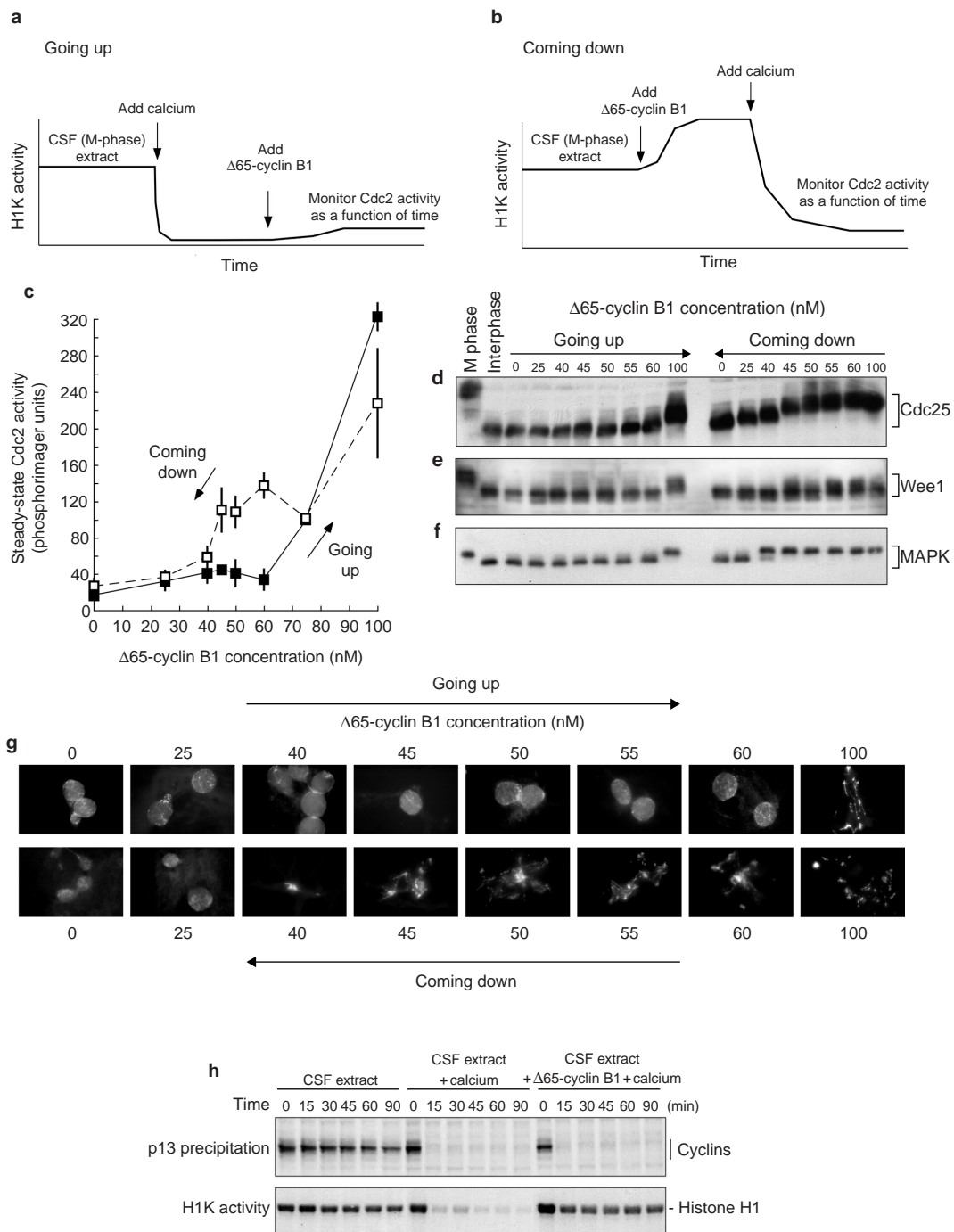


Figure 3 Hysteresis in the response of Cdc2 to cyclin, part 1. **a**, Interphase extracts were treated with recombinant $\Delta 65$ -cyclin B1 and allowed to reach steady-state ('going up'). **b**, Alternatively, CSF extracts were treated with recombinant $\Delta 65$ -cyclin B1 and then with 1 mM calcium to trigger degradation of the endogenous cyclin. Extracts were then allowed to reach steady-state ('coming down').

c, Hysteresis in steady-state histone H1 kinase activity. Filled squares represent extracts going up from interphase to M phase; open squares represent extracts coming down from M phase to interphase. **d-g**, Cdc25 hyperphosphorylation (**d**)

Wee1 hyperphosphorylation (**e**), p42 MAPK phosphorylation (**f**) and nuclear morphology (**g**). The data in **d-g** were derived from one experiment; the data in **c** are means \pm s.e.m. from three experiments. **h**, Calcium-triggered degradation of endogenous cyclins. The top panel shows an autoradiograph of p13 Suc1-precipitated ^{35}S -labelled endogenous cyclins in a CSF extract, a CSF extract treated with calcium, and a CSF extract treated with non-degradable $\Delta 65$ -cyclin B1 and then with calcium. The bottom panel shows the histone H1 kinase activities in the same samples.

interphase into the second mitotic M phase (the 'going up' extracts in this case; Fig. 4b) with the amount required to suppress exit from the first mitotic M phase (the 'coming down' extracts; Fig. 4c). We verified that both types of extracts approached steady-state levels of Cdc2 activity within 60–90 min of $\Delta 65$ -cyclin B1 addition (data

not shown). We then assessed Cdc2 activity (Fig. 4d), Cdc25 hyperphosphorylation (Fig. 4e), Wee1 hyperphosphorylation (Fig. 4f), p42 MAPK phosphorylation (Fig. 4g) and nuclear morphology (Fig. 4h) at steady state in the two types of extracts. We found that as little as 45 nM cyclin was sufficient to maintain the extracts in an

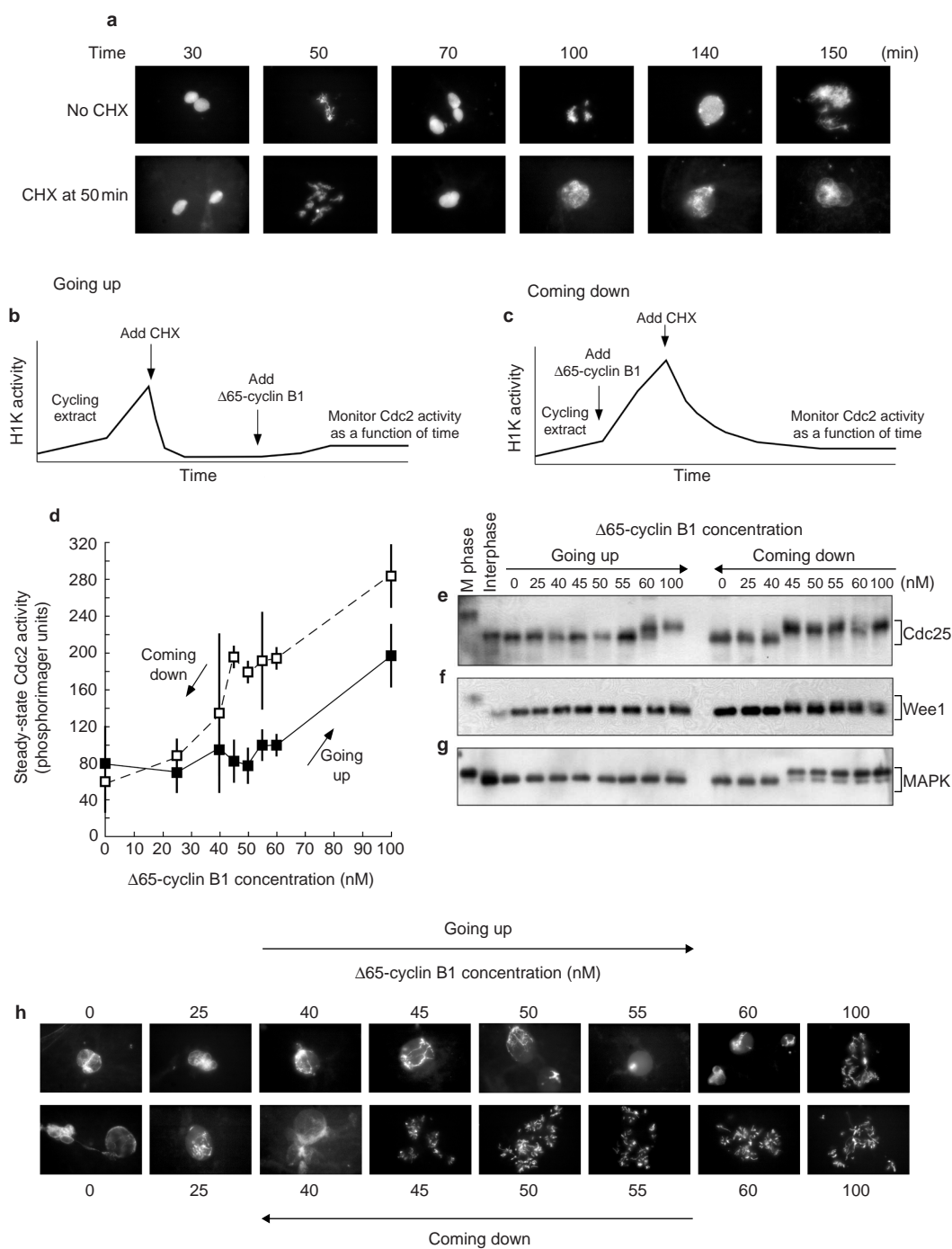


Figure 4 Hysteresis in the response of Cdc2 to cyclin, part 2. **a**, Nuclear morphology in cycling extracts (top) and in cycling extracts treated with cycloheximide at 50 min (bottom). **b**, Cycling *Xenopus* egg extracts were treated with cycloheximide at the time of the first mitotic M phase (50 min) and with recombinant $\Delta 65$ -cyclin B1 (30 min later). The extracts were then allowed to reach steady-state (going up). **c**, Alternatively, cycling were treated with recombinant $\Delta 65$ -cyclin B1 before the first mitotic M phase and were then treated with cycloheximide (at 50 min) to allow

degradation of the endogenous cyclin and to ensure that cyclin was not resynthesized (coming down). **d**, Hysteresis in steady-state histone H1 kinase activity. Filled squares represent extracts going up from interphase to M phase; open squares represent extracts coming down from M phase to interphase. **e–h**, Hysteresis in Cdc25 hyperphosphorylation (**e**), Wee1 hyperphosphorylation (**f**), p42 MAPK phosphorylation (**g**) and nuclear morphology (**h**). The data in **e–h** were derived from one experiment; the data in **d** are means \pm s.e.m. from two experiments.

M-phase-like state indefinitely, with high Cdc2 activity, hyperphosphorylated Cdc25, Wee1 and p42 MAPK, and condensed chromatin (Fig. 4d–h, ‘coming down’). In contrast, at least 60 nM cyclin was required to drive the interphase extracts into M phase (Fig. 4d–h, ‘going up’). Control experiments with ^{35}S -methionine

labelling and Suc1 precipitation established that the difference in thresholds could not be attributed to differences in the levels of endogenous cyclins (data not shown). Thus, these extracts exhibit hysteresis in their responses to $\Delta 65$ -cyclin B1 and hysteresis seems to be a general feature of Cdc2 activation and inactivation.

In summary, the Cdc2 activation system in *Xenopus* egg extracts is bistable: Cdc2 exhibits responses that are temporally abrupt, highly switch-like in steady-state terms, and, most importantly, characterized by biochemical hysteresis. The bistability of the mitotic trigger may allow the negative feedback loop of Cdc2 and the APC to exhibit sustained oscillations and function as a relaxation oscillator. These findings illustrate how two biochemical circuit elements with distinctive properties — a bistable positive feedback system (which alone behaves like a toggle switch) and a negative feedback loop (which alone behaves like an adaptational or homeostatic mechanism) — can combine to yield a third, distinct type of behaviour: the self-sustaining, spike-like oscillations of a relaxation oscillator.

Bistability is one mechanism to ensure that a biochemical oscillator produces sustained, rather than damped, oscillations. As mentioned above, a sufficiently long negative feedback loop may still be able to produce sustained oscillations in the absence of bistability^{12,25}. However, it seems that the combination of bistability and negative feedback may be a recurring motif in naturally occurring biological oscillators. For example, the mechanism that underlies the autonomous oscillations of cardiac pacemaker cells is analogous to the Cdc2 oscillator: the positive feedback in the opening of sodium channels corresponds to bistable activation of Cdc2 and the auto-inactivation of the sodium channel corresponds to APC-mediated cyclin degradation. Intracellular calcium oscillations have also been proposed to arise from combinations of bistability and negative feedback²⁷. Several aspects of *Saccharomyces cerevisiae* cell cycle regulation seem to be driven by combinations of positive and negative feedback loops, and there appears to be hysteresis in accumulation of the B-type cyclin Clb2 in *S. cerevisiae*²⁸, raising the possibility that the cell cycle includes multiple, inter-linked relaxation oscillators. A hysteresis-based oscillator may drive circadian rhythms¹⁵, with the comparatively slow pace of this oscillator arising out of its reliance on transcriptional changes. The fact that nature has converged on the same basic systems-level logic to produce oscillatory circuits out of very different types of signalling proteins in very different biological contexts argues that the positive feedback/negative feedback relaxation oscillator may be a particularly evolvable, reliable, or otherwise advantageous way of building biological clocks. □

Methods

Recombinant $\Delta 65$ -cyclin B1

The cDNA for an amino-terminal truncation of *Xenopus* cyclin B1 lacking the destruction box ($\Delta 65$ -cyclin B1) was subcloned into pRSET B (Invitrogen, Carlsbad, CA). $\Delta 65$ -cyclin B1 protein was expressed and purified essentially as described²⁹, except that inclusion bodies were resuspended in 6 M guanidine and the hexahistidine-tagged protein was enriched using a cobalt affinity resin (Clontech, Palo Alto, CA) and then eluted according to manufacturer's specifications. Selected fractions were pooled and dialysed²⁹ and the final protein concentration was determined by electrophoresis, Coomassie staining, gel scanning, and linear regression analysis using bovine serum albumin as a standard.

Xenopus egg extracts

Interphase cytosol and demembrated sperm chromatin were prepared as described previously²⁰. Steady-state responses and time-course experiments were performed in triplicate using interphase extracts. Hysteresis experiments were performed in duplicate or triplicate in two types of extracts, CSF extracts and cycling extracts, prepared essentially as previously described²⁶. The CSF extracts were prepared from unactivated eggs in the presence of 100 $\mu\text{g ml}^{-1}$ cycloheximide and then treated in one of two ways. First, the extracts were incubated for 30 min at room temperature with 1 mM calcium chloride to initiate cyclin destruction and drive the extract into an interphase state. Various concentrations of $\Delta 65$ -cyclin B1 were then added. Alternatively, various concentrations of $\Delta 65$ -cyclin B1 were incubated with the CSF extract for 30 min before addition of 1 mM calcium chloride to selectively degrade the endogenous cyclin. Cycling extracts were prepared from dejellied eggs treated with calcium ionophore A23187 (Sigma, St Louis, MO).

Samples of egg extracts were removed at intervals up to 90 min and frozen on dry ice for subsequent histone H1 kinase assays³⁶. Histone H1 kinase assay samples were electrophoresed through 10% SDS-polyacrylamide gels and blotted onto PVDF (Amersham Pharmacia Biotech, Piscataway, NJ). ³²P-labelled histone was detected by autoradiography (Biomax MR film; Kodak, Rochester, NY) and quantified by phosphorimaging. In some experiments, proteins were metabolically labelled *in extracto* with ³⁵S-methionine (0.9 $\mu\text{Ci } \mu\text{l}^{-1}$; Amersham Pharmacia Biotech) and labelled cyclin proteins were detected by p13 Suc1 precipitation and autoradiography. Nuclear envelope breakdown (NEBD) was assayed by including demembrated sperm chromatin in the extracts (1,000 sperm μl^{-1}) and then staining the chromatin with DAPI and assessing morphology by fluorescence and phase microscopy.

Immunoblots

Samples of egg extract were separated through a 10% 100:1 acrylamide-bisacrylamide gel, blotted onto PVDF and probed with rabbit polyclonal antibodies to Cdc25C (Zymed, San Francisco, CA), Wee1

(Zymed) or p42 MAPK (antiserum DC3, raised in our laboratory). Antibody concentrations were 0.5 $\mu\text{g ml}^{-1}$ for Cdc25C, 1 $\mu\text{g ml}^{-1}$ for Wee1 and 20 $\mu\text{g ml}^{-1}$ for p42 MAPK. The washed blot was then probed with donkey anti-rabbit horseradish peroxidase-conjugated secondary antibody (0.2 $\mu\text{g ml}^{-1}$; Amersham Pharmacia Biotech) and treated with ECL Plus chemiluminescent substrate (Amersham Pharmacia Biotech), or probed with goat anti-rabbit alkaline phosphatase-conjugated secondary antibody (0.2 $\mu\text{g ml}^{-1}$; Sigma) and treated with CDP-Star chemiluminescent substrate (Perkin-Elmer, Norwalk, CT). Biomax MR film was exposed to all blots and developed.

RECEIVED 6 JANUARY 2003; ACCEPTED 4 FEBRUARY 2003;
PUBLISHED 10 MARCH 2003.

- Hara, K., Tydemann, P. & Kirschner, M. A cytoplasmic clock with the same period as the division cycle in *Xenopus* eggs. *Proc. Natl Acad. Sci. USA* **77**, 462–466 (1980).
- Evans, T., Rosenthal, E. T., Youngblom, J., Distel, D. & Hunt, T. Cyclin: a protein specified by maternal mRNA in sea urchin eggs that is destroyed at each cleavage division. *Cell* **33**, 389–396 (1983).
- Murray, A. W. & Kirschner, M. W. Cyclin synthesis drives the early embryonic cell cycle. *Nature* **339**, 275–280 (1989).
- Masui, Y. & Markert, C. L. Cytoplasmic control of nuclear behaviour during meiotic maturation of frog oocytes. *J. Exp. Zool.* **177**, 129–145 (1971).
- Kumagai, A. & Dunphy, W. G. Regulation of the Cdc25 protein during the cell cycle in *Xenopus* extracts. *Cell* **70**, 139–151 (1992).
- Izumi, T., Walker, D. H. & Maller, J. L. Periodic changes in phosphorylation of the *Xenopus* Cdc25 phosphatase regulate its activity. *Mol. Biol. Cell* **3**, 927–939 (1992).
- Hoffmann, I., Clarke, P. R., Marcote, M. J., Karsenti, E. & Draetta, G. Phosphorylation and activation of human Cdc25-C by Cdc2-cyclin B and its involvement in the self-amplification of MPF at mitosis. *EMBO J.* **12**, 53–63 (1993).
- Tang, Z., Coleman, T. R. & Dunphy, W. G. Two distinct mechanisms for negative regulation of the Wee1 protein kinase. *EMBO J.* **12**, 3427–3436 (1993).
- Mueller, P. R., Coleman, T. R. & Dunphy, W. G. Cell cycle regulation of a *Xenopus* Wee1-like kinase. *Mol. Biol. Cell* **6**, 119–134 (1995).
- McGowan, C. H. & Russell, P. Cell cycle regulation of human WEE1. *EMBO J.* **14**, 2166–2175 (1995).
- Mueller, P. R., Coleman, T. R., Kumagai, A. & Dunphy, W. G. Myt1: a membrane-associated inhibitory kinase that phosphorylates Cdc2 on both threonine-14 and tyrosine-15. *Science* **270**, 86–90 (1995).
- Novak, B. & Tyson, J. J. Numerical analysis of a comprehensive model of M-phase control in *Xenopus* oocyte extracts and intact embryos. *J. Cell Sci.* **106**, 1153–1168 (1993).
- Thron, C. D. A model for a bistable biochemical trigger of mitosis. *Biophys. Chem.* **57**, 239–251 (1996).
- McMillen, D., Kopell, N., Hasty, J. & Collins, J. J. Synchronizing genetic relaxation oscillators by intercell signalling. *Proc. Natl Acad. Sci. USA* **99**, 679–684 (2002).
- Vilar, J., Kueh, H., Barkai, N. & Leibler, S. Mechanisms of noise-resistance in genetic oscillators. *Proc. Natl Acad. Sci. USA* **99**, 5988–5992 (2002).
- Goldbeter, A. Computational approaches to cellular rhythms. *Nature* **420**, 238–245 (2002).
- Tyson, J. J., Csikasz-Nagy, A. & Novak, B. The dynamics of cell cycle regulation. *BioEssays* **24**, 1095–1109 (2002).
- Reynhout, J. K. & Smith, L. D. Studies on the appearance and nature of a maturation-inducing factor in the cytoplasm of amphibian oocytes exposed to progesterone. *Dev. Biol.* **38**, 394–400 (1974).
- Schorderet-Slatkine, S. Action of progesterone and related steroids on oocyte maturation in *Xenopus laevis*. *An in vitro study. Cell Differ.* **1**, 179–189 (1972).
- Solomon, M. J., Glotzer, M., Lee, T. H., Philippe, M. & Kirschner, M. W. Cyclin activation of p34^{cdc2}. *Cell* **63**, 1013–1024 (1990).
- Abrieu, A. et al. The Polo-like kinase Plx1 is a component of the MPF amplification loop at the G2/M-phase transition of the cell cycle in *Xenopus* eggs. *J. Cell Sci.* **111**, 1751–1757 (1998).
- Qian, Y. W., Erikson, E., Taieb, F. E. & Maller, J. L. The polo-like kinase Plx1 is required for activation of the phosphatase Cdc25C and cyclin B–Cdc2 in *Xenopus* oocytes. *Mol. Biol. Cell* **12**, 1791–1799 (2001).
- Ferrell, J. E. Self-perpetuating states in signal transduction: positive feedback, double-negative feedback and bistability. *Curr. Opin. Cell Biol.* **14**, 140–148 (2002).
- Goldbeter, A. & Koshland, D. E. Jr An amplified sensitivity arising from covalent modification in biological systems. *Proc. Natl Acad. Sci. USA* **78**, 6840–6844 (1981).
- Goldbeter, A. A minimal cascade model for the mitotic oscillator involving cyclin and Cdc2 kinase. *Proc. Natl Acad. Sci. USA* **88**, 9107–9111 (1991).
- Murray, A. W. Cell cycle extracts. *Methods Cell Biol.* **36**, 581–605 (1991).
- Meyer, T. & Stryer, L. Molecular model for receptor-stimulated calcium spiking. *Proc. Natl Acad. Sci. USA* **85**, 5051–5055 (1988).
- Cross, F. R., Archambault, V., Miller, M. & Klovstad, M. Testing a mathematical model of the yeast cell cycle. *Mol. Biol. Cell* **13**, 52–70 (2002).
- Glotzer, M., Murray, A. W. & Kirschner, M. W. Cyclin is degraded by the ubiquitin pathway. *Nature* **349**, 132–138 (1991).
- Smythe, C. & Newport, J. W. Systems for the study of nuclear assembly, DNA replication, and nuclear breakdown in *Xenopus laevis* egg extracts. *Methods Cell Biol.* **35**, 449–468 (1991).

ACKNOWLEDGEMENTS

We thank H. Hochegger and T. Hunt for generously providing cyclin B1 antibodies, B. Dunphy for providing a cyclin B1 clone, S. Walter for constructing the $\Delta 65$ -cyclin B1 clone, T. Guadagno and S. Guadagno for producing and providing the Cdc25 and Wee1 antibodies, M. Hekmat-Nejad for advice on extract preparation, D. Gong for help with experiments, O. Brandmann, B. Novak, W. Sha, J. Sible and J. Tyson for helpful discussions, and K. Cimprich and members of the Ferrell laboratory for comments on the manuscript. This work was supported by the National Institutes of Health (grants GM61276 and GM46383).

Correspondence and requests for material should be addressed to J.F.

Supplementary Information accompanies the paper at www.nature.com/naturecellbiology.

COMPETING FINANCIAL INTERESTS

The authors declare that they have no competing financial interests.

Supplementary Materials, Part I. Global stability of a two-variable negative feedback system

We use the constants a and b to denote the total concentrations A_{tot} and B_{tot} respectively, so that $A(t) + A^*(t) \equiv a$ and $B(t) + B^*(t) \equiv b$, and introduce two variables x and y corresponding to the concentrations of activated forms A^* and B^* respectively. Using dots to denote time derivatives, we arrive to the the following system of ordinary differential equations:

$$\begin{aligned}\dot{x} &= -K(x) + (a - x)G(y) \\ \dot{y} &= -H(y) + (b - y)F(x).\end{aligned}$$

The functions K and H account for the constitutive transformation of A^* to A and B^* to B respectively, and we assume that $K(0) = 0$ and $H(0) = 0$ (that is to say, there is no degradation when concentrations are zero). We also make the assumption that K and H are strictly increasing differentiable functions. (Typical examples would be $K(x) = cx$, for some constant c , or $K(x) = \frac{cx}{d+x}$ for some constants c and d . Observe that, in general, the property $K(0) = 0$ means that we could also express K in the factored form $K(x) = xk(x)$, and similarly we could exhibit $H(y)$ in factored form.)

The functions $G(y)$ and $F(x)$ will be assumed to be positive for all values x and y ; furthermore, we will assume that G is a decreasing function and F is an increasing function: $G'(y) < 0$ and $F'(x) > 0$, corresponding to the requirements that y inhibits x and x activates y . Typical examples of such F, G are $F(x) = \frac{cx^n}{d^n+x^n}$ and $G(y) = \frac{c}{d^n+y^n}$, for suitable coefficients c, d, n .

We will now prove this theorem:

Theorem. *There is a unique steady state (\bar{x}, \bar{y}) , and this steady state is a globally asymptotically stable point for the above system of equations.*

We first need two simple observations:

Lemma 1. For each y in the range $0 \leq y \leq b$, there is a unique $x = Q(y)$ in the range $0 \leq x \leq a$ such that $-K(x) + (a - x)G(y) = 0$. Moreover, the function $y \mapsto Q(y)$ is a continuous and decreasing function.

Proof. Pick any y and denote $r = G(y)$. We need to show that there is some point $0 \leq x \leq a$ such that

$$K(x) = (a - x)r.$$

The right-hand side of this equality describes the line $L_r(x) = (a - x)r$, which has $L_r(0) = ar$ and $L_r(a) = 0$. The left-hand side, on the other hand, describes a function which has $K(0) = 0$ and increases as x ranges from 0 to a . Thus there must be an intersection point between graphs of L_r and K , corresponding to the desired point $x = Q(y)$. Moreover, as y increases, the negative slope $-r = -G(y)$ of the line L_r increases towards zero (because G is a decreasing function of y , by hypothesis), so the x -coordinate of the intersection point with the graph of $K(x)$ decreases; this proves that Q is a decreasing function, and Q is continuous because K is. By the Implicit Function Theorem, applied to the equation $-K(x) + (a - x)G(y) = 0$, one may moreover compute the derivative of Q :

$$Q'(y) = \frac{(a - x)G'(y)}{K'(x) + G(y)}.$$

Note that $K'(x) \geq 0$, $G(y) > 0$, and $G'(y) \leq 0$ so that, indeed, $Q'(y) \leq 0$.

An entirely analogous argument establishes the following:

Lemma 2. For each x in the range $0 \leq x \leq a$, there is a unique $y = P(x)$ in the range $0 \leq y \leq b$ such that $-H(y) + (b - y)F(x) = 0$. Moreover, the function $x \mapsto P(x)$ is a continuous and increasing function.

We are now ready to prove the existence and uniqueness of equilibria for our system. We must show that there is a unique pair (\bar{x}, \bar{y}) (in the ranges $0 \leq x \leq a$ and $0 \leq y \leq b$) such that both these equations hold:

$$\begin{aligned} -K(x) + (a - x)G(y) &= 0 \\ -H(y) + (b - y)F(x) &= 0. \end{aligned}$$

Equivalently, we need to show that there is a unique pair (\bar{x}, \bar{y}) such that both these equations hold:

$$\begin{aligned} x &= Q(y) \\ y &= P(x). \end{aligned}$$

Since P and Q are increasing and decreasing continuous functions, respectively, a unique intersection point exists (see Figure 1).

The Jacobian matrix of the system, evaluated at a generic point (x, y) is:

$$A(x, y) = \begin{pmatrix} -K'(x) - G(y) & (a - x)G'(y) \\ (b - y)F'(x) & -H'(y) - F(x) \end{pmatrix}.$$

Its determinant and trace are:

$$\begin{aligned} \det A(x, y) &= [K'(x) + G(y)][H'(y) + F(x)] - (a - x)(b - y)F'(x)G'(y) \\ \text{tr } A(x, y) &= -K'(x) - G(y) - H'(y) - F(x). \end{aligned}$$

The properties $K'(x) \geq 0$, $H'(y) \geq 0$, $G(y) > 0$, and $F(x) > 0$ imply that $\text{tr } A(x, y) < 0$ for all x, y . Similarly, $G'(y) \leq 0$ and $F'(x) \geq 0$, together with $a - x \geq 0$ and $b - y \geq 0$ imply that $\det A(x, y) > 0$ for all x, y .

In particular, then, evaluating at the equilibrium $(x, y) = (\bar{x}, \bar{y})$ these properties show that all eigenvalues of A have negative real parts. This shows the *local* stability of the equilibrium (\bar{x}, \bar{y}) .

The condition $\text{tr } A(x, y) < 0$ for all x, y says that the *divergence* of the vector field describing the system is always negative. This rules out periodic orbits in the system (Bendixson's criterion).

The Poincaré-Bendixson Theorem can now be applied. This theorem guarantees that all trajectories starting in the invariant region given by the square $[0, a] \times [0, b]$ converge to either: (1) a periodic orbit, (2) a homoclinic or heteroclinic connection, or (3) an equilibrium point. In our system, case (1) is ruled out by Bendixson's criterion, and case (2) is ruled out by the fact that the unique equilibrium is locally stable. Thus every trajectory must converge to (\bar{x}, \bar{y}) , and the proof of our theorem is complete.